Cement and Concrete Research 39 (2009) 417–425

Contents lists available at ScienceDirect

Cement and Concrete Research

journal homepage: http://ees.elsevier.com/CEMCON/default.asp

The physical and chemical characteristics of the shell of air-entrained bubbles in cement paste

M. Tyler Ley [a,*], Ryan Chancey [b], Maria C.G. Juenger [c], Kevin J. Folliard [c]

[a] Oklahoma State University, Stillwater OK, 74078, United States
[b] Nelson Architectural Engineers, Plano TX, 75093, United States
[c] The University of Texas at Austin, Austin TX, 78712, United States

ARTICLE INFO

Article history:
Received 5 February 2008
Accepted 30 January 2009

Keywords:
Freezing and thawing (C)
Admixture (D)
Fresh concrete (A)
Air entrainment

ABSTRACT

Recent research has suggested that the shell of an air-entrained void is important for resisting coalescence between air-voids and diffusion of gas from the surrounding fluid. The current paper describes the physical and chemical properties of an air-void shell during the first 2 h of hydration and chemical characteristics at 60 days. Results from this research suggest that the air-void shells found in air-entrained paste have varied physical properties and the crystalline material of these shells is largely made up of fine cement particles during the first 2 h of hydration. Observations of paste at 60 days of hydration suggest that the shell is made up of calcium silicate hydrate (C–S–H) with a morphology different from that in the bulk paste.

1. Introduction

Air-entrainment is the primary method to provide resistance to damage from freezing and thawing and salt scaling in concrete in North America. These bubbles are typically 10 μm to 1 mm in diameter and are stabilized with a surfactant during the mixing process. Extensive research has been performed on the bulk properties of air-entrained concrete and the distribution and volume of air-entrained bubbles in response to common changes in the system such as changes in mixing temperature or pressure from pumping or the weight of other concrete during placement. However, very little work has been done to investigate the fundamental behavior and properties of an air-entrained void and its surrounding shell. These shells have been suggested by Ley et al. [1] to be important in resisting the diffusion of gas into an air-entrained void from the surrounding fluid. Diffusion of gas is important as it suggests that the small air-voids may diminish or decrease in size with time in fresh cement paste and lead to the increase in size of the more coarse air-voids and total volume of air [2].

This phenomenon could explain the occasional discrepancy between the measurements of the total volume of fresh and hardened air content as reported by several researchers [3,4].

The goal of the present study was to investigate possible changes in air-void size and volume in fresh paste as suggested by Mielenz et al. [2]. A further goal was to characterize the nature of the air-void shell that governs this behavior. This paper presents investigations of the relevant physical properties of air-entrained voids and their response to outside stress. Furthermore, x-ray diffraction (XRD), scanning electron microscopy (SEM), and energy-dispersive x-ray analysis (EDXA) are used to determine the chemical properties and morphology of the air-void shell at times of less than 2 h and at 60 days.

1.1. Background

In some of the earliest work done to investigate the fundamental characteristics of an air-void system in concrete, Mielenz et al. [2] photographed air-entrained voids in dilute pastes (i.e. high water-to-cementitious material ratio (w/cm)) with the aid of an optical microscope. These pictures showed that the perimeter of the air-entrained voids was covered by an early hydration shell. It was suggested that these shells could be made up of either a precipitated solid or gelatinous film from the calcium salts of the air-entraining agent (AEA) or metal ions contributed from the hydrating cement paste. The mechanism suggested by Mielenz et al. [2] to describe the shell formation is that the calcium salts of the AEA are soluble when the material is mixed in the bulk paste but could precipitate once concentrated around the air–water interface. To demonstrate this behavior, common AEAs were mixed with saturated lime-water and a white and brown insoluble precipitate formed. It was suggested that this insoluble material comprises the air-void shells. Mielenz et al. [2] also observed that cement particles were attracted to the surface of the air-entrained void.

Dodson [5] pointed out that all commercially available AEAs are anionic in nature. This suggests that the hydrophilic portions of the surfactant molecules align themselves preferentially around the perimeter of an air-void and that these molecules are negatively charged. Dodson also suggested that the calcium ions, with their high

* Corresponding author.
E-mail address: tyler.ley@okstate.edu (M.T. Ley).

0008-8846/$ – see front matter © 2009 Published by Elsevier Ltd.
doi:10.1016/j.cemconres.2009.01.018

Table 1
Summary of the RQXRD analysis for the air-void shells and bulk paste.

	Time	C_2S %	C_4AF %	C_3A %	$CaCO_3$ %	C_3S %	Ettringite %	Gypsum %	Sum %
Wood rosin	0	15.7	8.7	2.7	2.6	68.0	0.8	1.3	99.8
	8	17.6 (0.8)	13.6 (1.2)	5.6 (0.9)	8.0 (0.8)	50.5 (2.4)	2.6 (2.1)	2.0 (1.4)	100.0
	30	20.9	16.4	4.3	12.7	38.2	5.3	2.2	100.0
	45	18.9 (4.0)	14.7 (0.6)	5.8 (1.6)	14.7 (3.0)	41.6 (0.4)	1.3 (0.3)	3.2 (0.1)	100.1
	90	20.7 (1.5)	16.5 (0.5)	5.5 (1.2)	14.1 (0.9)	38.3 (0.5)	2.2 (2.5)	2.8 (0.4)	100.0
	120	22.5 (3.9)	16.5 (1.6)	5.2 (1.2)	14.6 (2.7)	35.5 (6.5)	4.1 (3.3)	1.6 (0.8)	100.0
Synthetic	0	15.7	8.7	2.7	2.6	68.0	0.8	1.3	99.8
	8	18.2 (0.2)	18.8 (2.7)	4.7 (0.4)	21.9 (5.7)	33.1 (9.5)	0.9 (0.4)	2.4 (1.0)	100.0
	30	16.0 (0.7)	14.6 (1.4)	6.6 (0.4)	20.8 (3.9)	36.1 (5.5)	3.8 (0.1)	2.1 (1.2)	100.0
	45	15.4 (0.4)	18.0 (5.8)	5.0 (1.3)	18.6 (6.2)	38.7 (12.8)	1.7 (1.1)	2.7 (2.8)	100.0
	60	18.7 (3.9)	15.8 (2.1)	5.0 (1.2)	18.0 (8.0)	38.5 (8.1)	3.0 (1.2)	1.1 (0.5)	100.1
Bulk paste	0	15.7	8.7	2.7	2.6	68.0	0.8	1.3	99.8
	10	10.1	7.1	2.7	4.7	67.7	2.6	5.1	100.0
	45	13.0 (3.7)	8.2 (0.9)	2.9 (1.2)	6.4 (2.5)	60.3 (1.4)	1.6 (0.5)	7.6 (2.4)	100.0
	90	13.7	8.7	3.8	6.6	60.0	1.6	5.6	99.9
	120	13.6	12.5	4.2	4.7	58.4	0.7	6.0	100.0

The values at 0 min of hydration correspond to the unhydrated cement. All values shown are the percentage of crystalline material analyzed. The standard deviation is shown in parentheses.

charge density, are attracted to the negatively charged, hydrophobic ions stabilizing the bubble and these react to form an insoluble calcium salt, which was suggested to be a calcium rosinate. However, Dodson did not provide any experimental evidence to support this hypothesis. A study by Pigeon and Plante [6] that utilized SEM with microprobe analysis on specimens prepared with high dosages of alkaline salts suggested that there were increased concentrations of sodium and potassium ions around air-entrained voids. The concentration was much larger than would be expected to be provided from the AEA and larger than that measured in the bulk cement paste. However, calcium ion concentration was not investigated in this study and the methods utilized did not allow observations of the bulk paste.

Several other studies investigated the mechanisms of freeze-thaw damage and the characteristics of air-void shells [7–9]. These studies featured samples whose hydration had been stopped by cryogenic freezing. The samples were then investigated in a low temperature scanning electron microscope (LTSEM). A technique was also developed that allowed the air-voids to be separated from the paste and then frozen and investigated with the LTSEM. Upon freezing, these air-voids were largely irregular in shape and seemed to be made up of heterogeneous fine particles that were between 1 and 5 μm. The researchers hypothesized that the particles surrounding the air-voids at least partially consist of unhydrated cement particles [9]. Observations were also made of the morphology and interface between the air-void shells and the bulk paste [7–9]. The hydration products were suggested to be very dense over the 1–2 μm shell and a 10–15 μm water-filled space or transition zone seems to exist between the shell and the bulk paste. This zone in some ways is similar to the zone observed between bulk paste and aggregate. This gap was reported to increase in size as the w/cm of the mixtures increased and decreased in size with increased hydration.

2. Experimental methods

In this study, several physical properties of the shells were investigated using a novel technique of isolating the bubbles in bleed water and then examining their response to stress. The behavior of the bubbles was captured with a digital camera fitted to a stereomicroscope at 500× magnification.

Chemical properties of the shell were also evaluated over the first 2 h of hydration and at 60 days of hydration with the use of XRD and SEM with EDXA. The goal of this study was to investigate the microstructure and composition of the air-void shell and how they change with time with the hopes that this would lead to a better understanding of the behavior of the air-void shell and how it can ultimately be improved.

All of the specimens in this study were produced with a 0.42 w/cm paste using 1.37 kg of cement meeting the ASTM C 150 [10] specifications for Type I and II with a 0.53 alkali content (Na_2Oeq). The phases of the cement were determined by Rietveld quantitative x-ray diffraction (RQXRD) [11,12] analysis and are reported in Table 1 as the specimens at 0 min of hydration. The mixer and mixing procedure used in this study met requirements of ASTM C 305 [13]. All other details of the specimens are given in the respective sections.

2.1. Physical properties

All of the observations of physical properties of the air-void shells were made by using a novel technique to investigate air-voids in the bleed water of cement paste contained in a bottle as shown in Fig. 1. More details can be found in Ley et al. [1]. A short summary of the experimental technique follows.

After the mixing of the paste was completed, a funnel was used to transfer the material into a transparent polystyrene bottle. The bottle was filled to capacity and the cap was tightened and the bottle was placed horizontally. After sitting for approximately 10 min it was possible to observe a layer of bleed water forming at the surface of the paste (Fig. 1). In this bleed water, air-voids could be found that had worked their way to the surface of the paste due to their buoyancy. These voids were then observed and documented using a

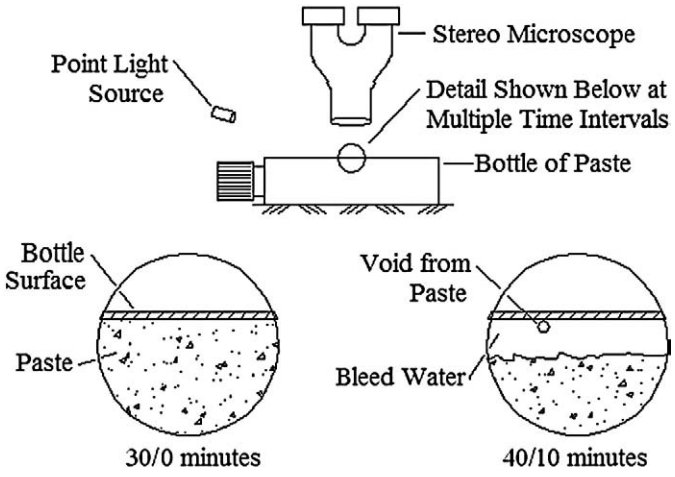

Fig. 1. The experimental setup for the physical testing showing the orientation of bottle, stereoscope, and point light source. The detailed cross-section is at two time intervals. The time is displayed in minutes after initial hydration/time after the bottle was placed on its side.

stereomicroscope fitted with a digital camera. A computer program was written to capture images of the changes in these voids at specified intervals of time.

For some of the specimens, the same preparation technique was used; but an air pump was attached to the bottle of paste with a pressure regulator and gage. This allowed the fluid pressure inside of the bottle to be increased or decreased in any manner while the bubbles were investigated with the stereomicroscope and digital camera. The air-voids were investigated while they were subjected to an increase and then decrease in fluid pressure.

With these experimental setups, the following physical properties of air-entrained bubbles were investigated: adhesion of cement particles, transparency, the response of bubbles to fluid pressure, and the ability of the air-void shell to repair after being damaged.

2.2. Chemical properties during the first 2 h of hydration

In order to determine the chemical consistency of the air-void shell, the air-voids were separated from the paste at different time periods, in this case from 8 min to 2 h of hydration by injecting a 20 cm^3 sample of air-entrained paste into the bottom of a tall column of water utilized by the Air-Void Analyzer (Germann Instruments) as this provided a useful method to liberate the bubbles from the paste. A stirring rod at the bottom agitated the paste and the bubbles rose up the column. The bubbles were caught at the top of the column with an inverted watch glass. After collecting bubbles for 3 min, the watch glass was removed. The majority of the bubbles collected adhered to the watch glass surface. The excess water was removed from the watch glass with a syringe and the specimen was placed in a vacuum desiccator overnight. The dried material was scraped from the watch glass and stored under vacuum until the crystalline material could be analyzed by RQXRD. Because so little material was collected during the bubble separation (approximately 5 mg) it was necessary to use a standard height low-background quartz-disk specimen holder. The specimen holder was covered with a thin layer of petroleum jelly to insure the material would adhere to the holder. The sample was sprinkled onto the jelly and then spread out so a thin layer of material covered the surface. Care was taken to ensure that a low profile of powder was used for the sample, such that proper specimen height was maintained, thus minimizing sample-displacement error. A sample holder was also analyzed that was only covered in petroleum jelly and was found to give only slight background noise at low angles of investigation. This was determined to not impact the accuracy of the quantitative analysis.

This technique was utilized to analyze air-voids from pastes containing wood rosin and synthetic AEA dosed at 48 mL/100 kg of cement at various time intervals, up to 2 h of hydration. A non air-entrained paste was also investigated after 30 min of hydration. The same cement was used for this testing as was used for examination of the physical properties of the air-voids.

The properties of the bulk cement paste were determined on samples of hydrated cement paste obtained from a paste containing 48 mL/100 kg of cement of a wood rosin AEA which was allowed to hydrate in the mixing bowl and was stirred by hand prior to a sample being extracted at time intervals of hydration from 8 min to 2 h. No petroleum jelly was used for this analysis as the paste was placed directly on the low-background sample holder at the reported time of hydration and then placed in a drying vacuum. It is unclear how long it took the water to be removed from the sample. While visual observations of the color change of the sample indicate that drying was complete within 5 min under vacuum, drying was allowed to continue overnight. A low-background sample holder was used so that the sample preparation between the two methods was kept as similar as possible. After the specimens were dried, the height of the sample was reduced to the clearance of the zero background sample holder in order to minimize the sample displacement.

Cement samples were also analyzed by preparing approximately 2 g of cement in a standard powder-mount sample holder. The RQXRD analysis was performed with a Siemens D500 x-ray diffractometer equipped with a DACO_MP digital controller and analog-to-digital signal converter. All samples were analyzed from 20° to 80° 2θ, with a step size of 0.02° and dwell time of 4 s/step. The atypically lengthy step provided a sufficient x-ray signal-to-noise ratio for rigorous quantitative analysis. A traditional 2200 W copper (Cu) x-ray tube was used. The diffractometer was configured with a 1° divergent slit, a 4° soller slit, and a 1° antiscatter slit on the incident-beam side. A 1° antiscatter slit, a 4° soller slit, a single-crystal monochromator, a

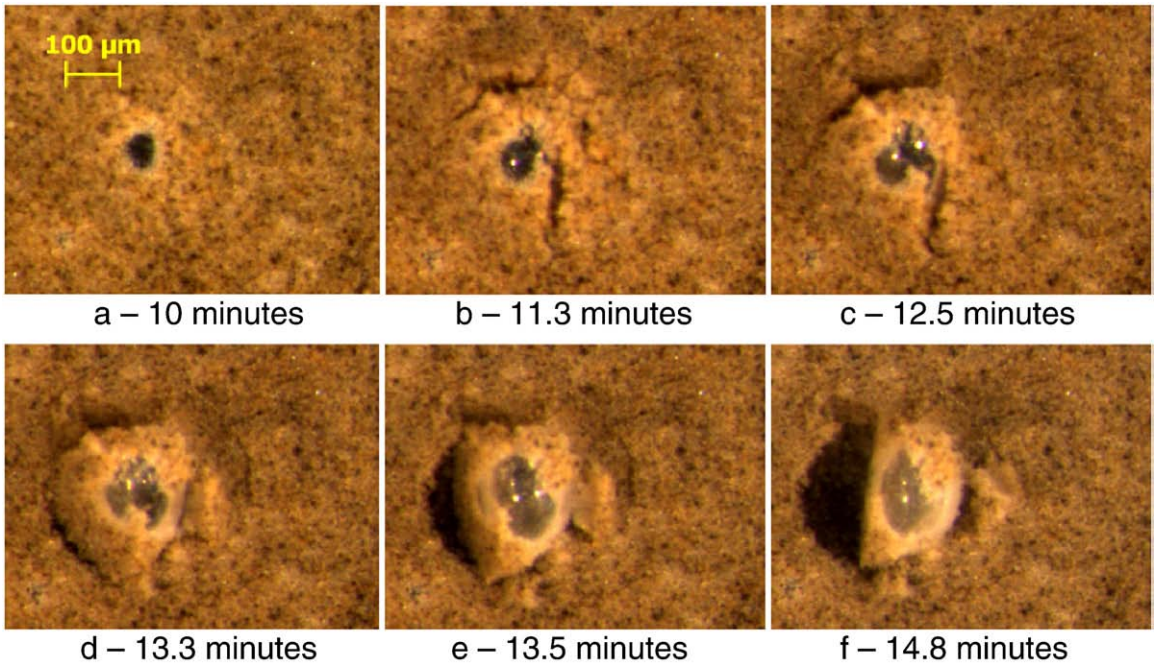

Fig. 2. An air-entrained void is shown emerging from a cement paste surface due to buoyancy with cement grains attached. The paste was made with 48 mL/100 kg of cm of a wood rosin AEA. Please see online supplementary data for more information.

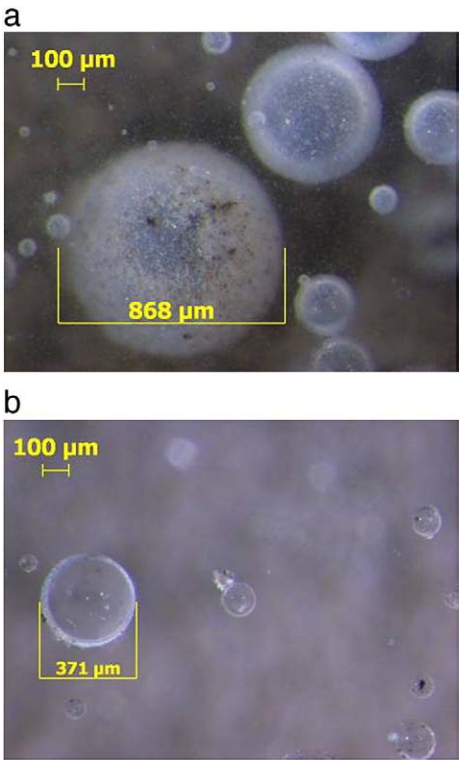

Fig. 3. a. Air-entrained void (48 mL/100 kg of cm wood rosin AEA) after 45 min of hydration. b. Non air-entrained voids after 45 min of hydration.

0.15 mm receiving slit, and a 0.6 mm detector slit were used on the divergent-beam side. Each pattern was analyzed using the whole-pattern fitting method developed by Rietveld [11] and demonstrated for use in cementitious materials by Stutzman [12] using the TOPAS-Academic software package.

2.3. Chemical properties after 60 days of hydration

Air-entrained paste made with wood rosin AEA at 48 mL/100 kg of cement was allowed to hydrate inside of a bottle shown in Fig. 1 in a 100% RH environment for 60 days. The sample was fractured and a small flake about 2 mm thick of the now exposed, interior surface was stored in a vacuum until it was examined with a SEM with EDXA. The SEM used was a LEO 1530 Field Emission SEM equipped with an IXRF solid-state energy dispersive spectrometer. The operating voltage was 15 kV, working distance = 11 mm, x-ray count rate = 400 cps, and EDXA dwell time = 60 s. The sample was sputter-coated with a 20 nm thick layer of silver to provide conductive continuity.

3. Results and discussion

3.1. Physical properties

3.1.1. Adhesion of cement particles

In Fig. 2, a paste made with wood rosin AEA at a dosage of 48 mL/100 kg of cement is shown after 10 min of hydration. When the void leaves the cement paste and rises to the surface, one can clearly see a significant portion of cement paste is adhering to the air-entrained void and is also carried up to the surface of the bottle. This implies that the attraction between the cement particles and the air-entrained bubble is significant. This observation is not an anomaly and the adhesion of cement to air-entrained bubbles is regularly observable in bubbles that initially emerge from the paste. Observations of these bubbles and bubbles that emerge from the paste after about 10 min suggest that the cement paste does not stay permanently affixed to the bubble surface. This observation confirms previous work by Mielenz et al. [2] and hypothesized by Corr et al. [9].

3.1.2. Transparency

Air-voids from a paste with wood rosin AEA used at a dosage of 48 mL/100 kg of cement are shown in Fig. 3a. The air-voids shown in Fig. 3b are from a paste with no AEA. Both pictures were taken

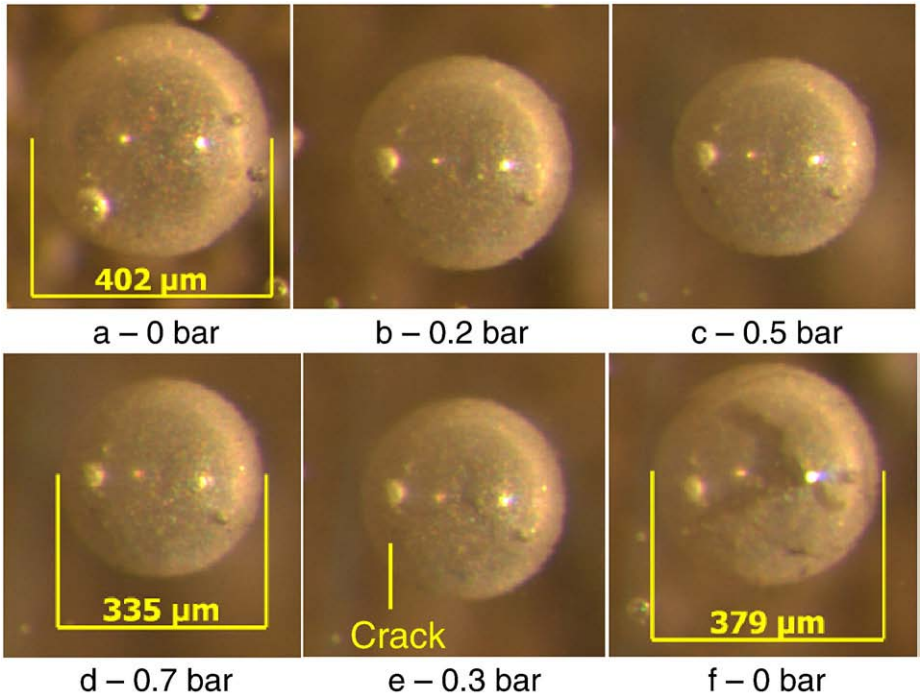

Fig. 4. The response of a mixture containing 26 mL/100 kg cm of Vinsol resin and 81 mL/100 kg of normal range water reducer subjected to a pressure 0.7 bar above atmospheric and then returned back to atmospheric pressure.

approximately 45 min after mixing. There is a significant difference in the transparency of the void wall in air-entrained and non air-entrained pastes, the former are translucent while the latter are transparent. In past literature bubbles in concrete have arbitrarily been categorized as either entrained (<1 mm) or entrapped (>1 mm) air due to their size. This definition does not seem to be useful in describing the observations in this paper. The observed difference in transparency is likely attributable to the shell material that has been shown to exist around voids in air-entrained paste and is missing from voids in a non air-entrained paste [1]. These shells seem to be present at AEA dosages typically used in concrete. The translucent air-void shells were regularly observed for the following AEAs: wood rosin, Vinsol resin, tall oil, and synthetics. The appearance of the shells is different for each of the AEAs. Little difference in appearance was observed for different dosages of AEA, but more work is needed in this area.

3.1.3. Bubble response to fluid pressure

3.1.3.1. Vinsol resin AEA. An air-void in the bleed water of an air-entrained paste with 26 mL/100 kg of Vinsol resin AEA and 81 mL/100 kg of a polymer-based normal range water reducer is shown at atmospheric pressure in Fig. 4a after 45 min of hydration. For this test, the fluid surrounding the air-void system was increased to 0.7 bar above atmospheric pressure in 10 equally spaced steps and then decreased back to atmospheric pressure in three equal steps. A selected number of images are shown in Fig. 4 with Fig. 4a–d showing the results of increasing pressure and Fig. 4e and F showing voids while the pressure is decreasing.

In Fig. 4d, one can see that the air-void has decreased in diameter by almost 20% at a pressure of 0.7 bar and yet the bubble does not appear to be damaged. As the pressure began to be released, it can be seen in Fig. 4e that the shell of the large air-void cracked as the volume of air increased inside the void. These cracks widen in Fig. 4f as the fluid was brought back to atmospheric pressure. This is significant as it has been previously shown by Ley et al. [1] that after the air-void shell has been damaged, it is possible for an interchange of air to occur from the surrounding fluid as seen by Mielenz et al. [2], then a change in the air-void distribution and volume can occur. It appears that some amount of air was lost to the surrounding fluid during the increase in fluid pressure as the final diameter is 6% lower than the initial diameter. It is likely that this volume of air has dissolved into the fluid surrounding the bubble. Similar behavior was found for voids of a similar size stabilized by wood rosin AEAs. This behavior has been witnessed regularly for voids that are larger than 200 μm. However, it is difficult to say whether the same shell damage occurs in voids that are smaller as they are difficult to observe at the magnification used. More than 150 different bubbles have been observed stabilized by wood rosin and Vinsol resin AEAs in this test setup.

3.1.3.2. Synthetic AEA. A void in the bleed water of air-entrained paste with 47 mL/100 kg dosage of a synthetic AEA and 85 mL/100 kg of normal range water reducer is shown in Fig. 5a after 45 min of hydration. The surrounding fluid pressure was increased to 0.7 bar in 5 equal pressure steps and then decreased back to atmospheric pressure in three equal pressure steps.

At a pressure of 0.3 bar, the shell of the air-entrained void began to distort as shown in Fig. 5b. As the fluid pressure increased, so did the distortion of the void. It can be seen in Fig. 5c that the bubble was no longer spherical and had a significant crease at the center. Whenever the air pressure was reduced back to atmospheric the shell returned to a size within 5% of the original diameter. Also, during this increase and decrease in pressure, the shell of the void was never observed to be damaged. This test was performed over 25 times and the behavior was similar for voids larger than 40 μm. Voids smaller than this did not appear to show the same buckling of the shell; but it was found to be difficult to observe small voids at this magnification.

3.1.3.3. Differences in AEAs. It is clear that there is a significant difference in behavior between the synthetic and the Vinsol resin and wood rosin AEAs. The air-void stabilized with the synthetic AEA seemed to buckle as the surrounding fluid pressure was increased. This seems to imply that the air-void shell has some stiffness in compression and a substantial amount of viscoplasticity in tension as

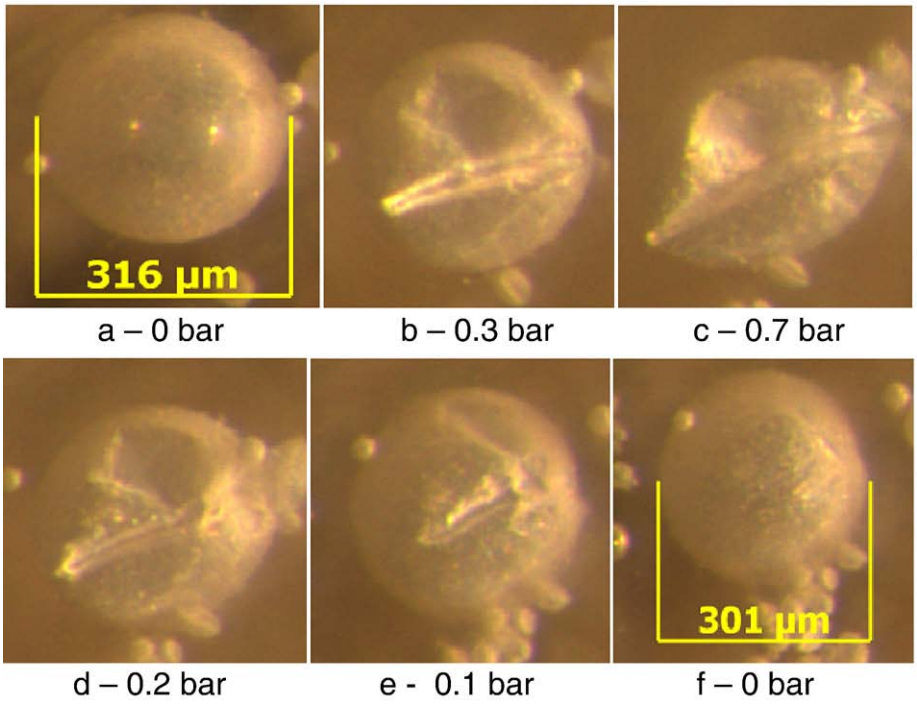

Fig. 5. The response of an air-entrained void in a mixture (47 mL/100 kg of cm of synthetic AEA and 81 mL/100 kg of normal range water reducer) subjected to a pressure 0.7 bar above atmospheric and then returned back to atmospheric pressure.

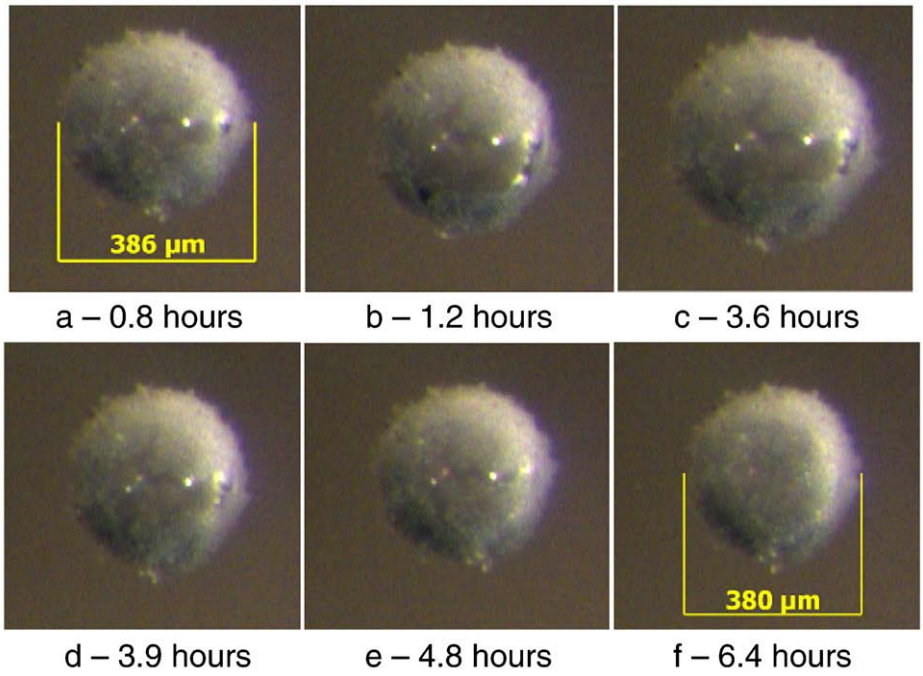

Fig. 6. A void in bleed water above a cement paste (48 mL/100 kg of cm of a wood rosin AEA) was subjected to a pressure 0.7 bar above atmospheric and then returned back to atmospheric pressure.

the void did not crack when the fluid returned to atmospheric pressure. On the other hand, the air-void stabilized with the Vinsol resin and appeared to resist the compressive strains without damage and yet seemed to be very weak in tension. This difference in behavior is possibly attributable to the difference in the molecular structure of the AEA or the resulting air-void shell, and thus the surrounding hydration products. A similar response to pressure as that witnessed with the synthetic surfactant has been observed in other research on surfactants and their response to pressure [14].

3.1.4. Self repairing

In Fig. 6 an air-void above a paste containing 48 mL/100 kg of wood rosin AEA that has been pressurized to 0.7 bar and then depressurized to atmospheric pressure is shown over a 5.7 hour time period. As stated previously, the shell of air-voids in wood rosin systems crack while being depressurized. Fig. 6a shows a void with a cracked shell immediately after the return to atmospheric pressure. Over the next 0.4 h the shell continues to crack and expose more of the underlying bubble, Fig. 6b. This occurred while the bottle sat undisturbed. At 3.6 h after hydration began, the shell around the air-void begins to reform, Fig. 6c. Pictures are shown of the shell reforming over the next 2.8 h. In Fig. 6f an image is shown after 6.4 h of hydration and it appears that the shell has repaired itself completely and no cracks are present.

If an air-void shell were able to self heal, then this behavior could provide a method for the air-void to recover from damage to the surrounding shell as previously shown with changes in pressure. One reason why the shell in Fig. 6 may have taken such a long period of time to repair itself was the large amount of damage that was done to it. If this damage had been less severe, then the repair might have taken less time. These observations may also help provide insight into the mechanisms of the initial air-void shell formation as they show nucleation and growth of the shell only at the interface between the bubble and the shell. Three other observations of self healing have been made but none as dramatic as the one shown in Fig. 6. On the majority of the tests completed it was difficult to observe the shells being repaired as the cracks in the bubbles are small and the repairs seem to take less time.

3.2. Chemical properties

3.2.1. Chemical properties during the first 2 h of hydration

Table 1 contains a summary of the crystalline material analyzed in the air-void shells in pastes containing wood rosin and synthetic AEAs over time. Table 1 also contains results from analysis of the crystalline materials in the bulk paste. The data for the unhydrated cement indicate the composition of the starting material. Repeat specimens were run for the majority of the data points and the values presented in Table 1 are averages with standard deviations in parentheses. While some variability was found, it was determined to not be significant for phases that were present in quantity greater than 10% of the overall crystalline material of the sample.

All of the specimens analyzed contained the same crystalline phases; however, the amount of each phase present in the sample varied with sample type and time. The results indicate that there is very little change in the crystalline phases present in the bulk cement paste over the first 2 h of hydration. This is not surprising since the onset of significant C_3S hydration is not expected in this time period at

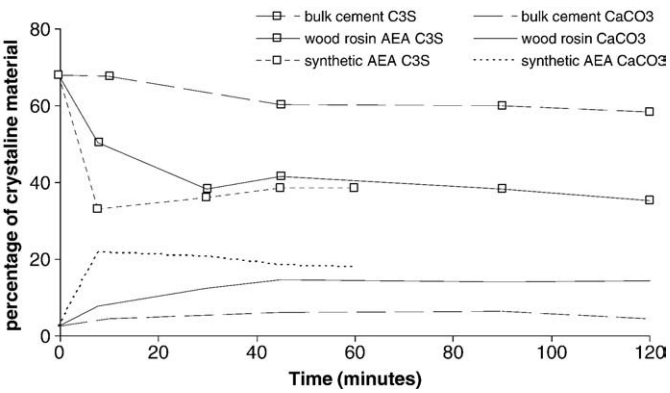

Fig. 7. Change in C_3S and $CaCO_3$ content with time is shown for the bulk cement paste and the air-void shells created with wood rosin and synthetic AEAs.

room temperature in the absence of accelerators. The changes in quantities of the other phases are within error and can be considered negligible.

For the specimens taken from the air-void shell material it was found that there was a significant change in the amounts of anhydrous material and $CaCO_3$ with time in the samples. The C_3S and $CaCO_3$ contents are shown graphically in Fig. 7. In each of the types of air-void shells it appears that there is less C_3S than in the bulk cement paste. In the wood rosin AEA shells, the C_3S content appears to decrease between 8 and 30 min, and then remains constant. In the synthetic AEA shell, the amount of C_3S decreases from the initial amount found in the cement and then is constant with time.

Correspondingly, the percentage of other crystalline phases present are observed to increase with time. This is expected if an accelerated dissolution of C_3S is occurring. Another interesting observation is that the amount of $CaCO_3$ is higher in the air-void shells than in the original cement and increases with time up to 30 min. After 30 min the amounts of $CaCO_3$ remain constant. The increase in $CaCO_3$ seems to occur at an increased rate when the specimen is made with the synthetic AEA compared to wood rosin AEA, but they reach the same constant level with time.

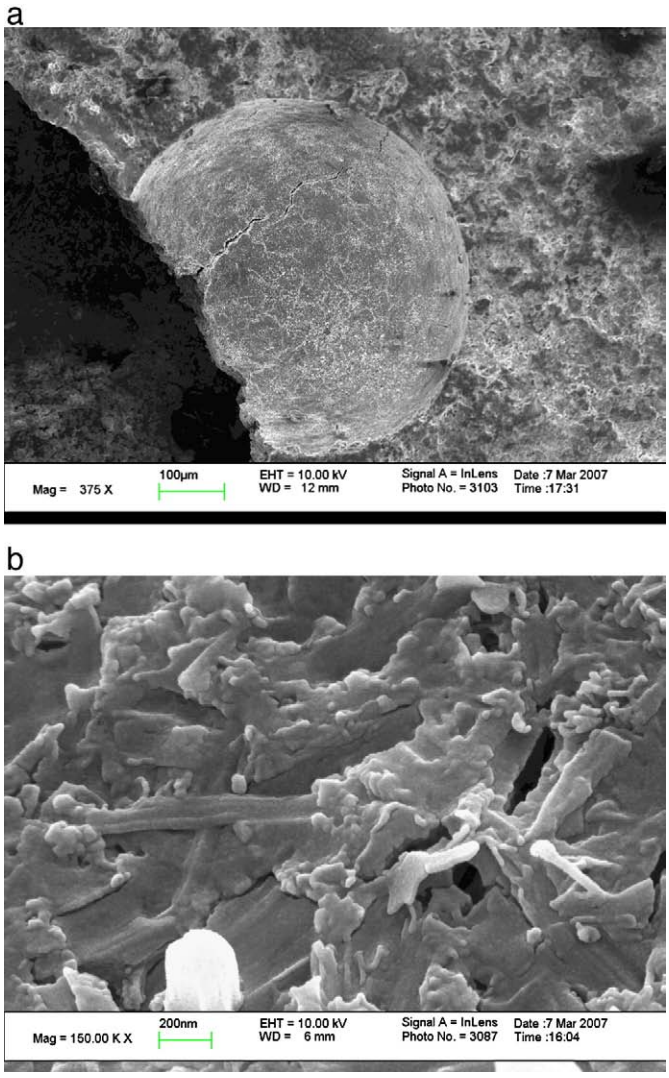

Fig. 8. SEM image of an air-entrained void from a mixture containing a wood rosin AEA at 48 mL/100 kg of cement that was allowed to hydrate for 60 days before examination. An overview of the void is shown in Fig. 8a. Fig. 8b shows the void surface under increased magnification.

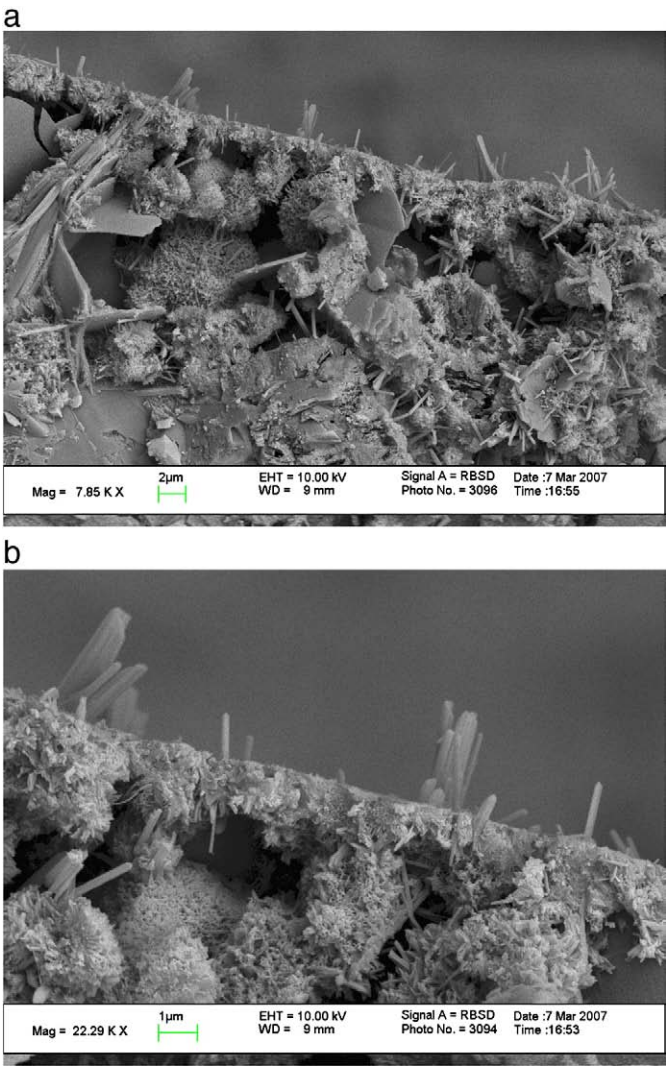

Fig. 9. An SEM image of the interface between the air-void in Fig. 8 and the bulk paste. In Fig. 9b a close up is shown of Fig. 9a.

The initial amount of $CaCO_3$ is likely filler added to the cement; however, the changes in anhydrous phases and the presence of so much $CaCO_3$ in the collected samples are unexpected. More discussion on these observations appears later in the paper. However, whatever the mechanism is for the increase in $CaCO_3$ is it is likely tied to the reduction in the C_3S as they are occur simultaneously and proportionately.

3.2.2. Chemical properties at 60 days of hydration

An air-entrained void approximately 550 µm in diameter was found on a fractured hardened cement paste surface previously discussed and investigated with a SEM with EDXA. A top view of the air-void is shown in Fig. 8a and magnified picture of the air-void wall is shown in Fig. 8b. The interface between the air-void shell and the bulk paste is shown in Fig. 9a and at increased magnification in Fig. 9b. From Fig. 9 it appears there is a 1 µm thick shell of hydration product is surrounding the air-void. Just adjacent to the shell there appears to be a discontinuity between the phases in the shell and the bulk paste of the sample, similar to the observations mentioned previously [7–9]. The shell seems to be made of a very dense hydration product. Furthermore, it seems small crystals are growing on the surface of the void. Visual and EDXA completed at high magnification suggest that these crystals are ettringite.

At the high magnification shown in Fig. 8b one is able to closely examine the very dense microstructure of the air-void shell. To investigate the chemical composition of the shell, an area of approximately 185 μm × 135 μm of the air-void shell was investigated with EDXA. Since this analysis is taken over a large area it should be representative of the chemical makeup of the void surface and some underlying material due to the size of the interaction volume. It was determined that the majority of the sample was made primarily of calcium and silicon. Trace amounts of aluminum and sulfur were also found. The ratio of calcium-to-silicon of the air-void shell was equal to 1.1. This is lower than what is expected for a typical C–S–H found in bulk cement paste. When the EDXA was used to investigate C–S–H found in the bulk paste of this sample, the calcium-to-silicon ratio was found to be 1.5. The ratio for the C–S–H of the bulk paste agrees with numbers given by Pigeon and Plante [6] and Diamond [15] for the method used.

EDXA seems to indicate that the air-void shells consist of C–S–H with small amounts of ettringite needles on the surface of the void. The air-void hydration shell shown in Fig. 9 seems to be denser than the C–S–H found in the bulk paste. This can be seen in Fig. 9 if one looks at the large number of voids in the hydration product formed adjacent to the shell in comparison to the shell itself. The shell thickness and presence of a "transition zone" supports results from Corr et al. [9].

4. Discussion of mechanisms

RQXRD showed that the early composition of the air void shell is very similar to the bulk cement paste but with a lower C_3S content, higher amounts of other anhydrous phases, and higher $CaCO_3$ content. These differences are unexpected and merit further discussion. The ability to understand the chemistry of these air void shells is critical in order to improve the performance of air entraining agents and understand the observed behavior.

The charge imparted by the anionic AEA on the outside of the air-entrained void may be significant in explaining the composition of the air void shell. This anionic charge likely contributes to the adhesion of cement particles to the air void. The surfaces of cement particles are charged, causing an attraction between the particles and the outside of the bubble. This attraction results in cement particles adhering to the bubble as shown in Fig. 2 and as suggested by others [2,9]. This also results in the high quantities of anhydrous cement phases measured in the bubble shell at early ages through RQXRD.

If the early hydration shell were made up completely of adhered cement particles, then the shell composition would be identical to the unhydrated cement and, correspondingly, the bulk paste since it does not differ significantly from the unhydrated cement at the times examined. However, the amount of C_3S in the shells is much lower than the amount of C_3S in the anhydrous cement and bulk paste. If all anhydrous phases were present in lower amounts in the shell, then one could assume that the ratio of cement-to-reaction products in the shell is lower than in the paste. However, the relative proportions of the other anhydrous phases are higher in the shell than in the original cement. One possible explanation for this difference is that the C_3S dissolves more rapidly in the cement particles attached to the air void. This explanation is consistent with the decrease in C_3S and increase in all other analyzed phases. Since all analyzed phases by RQXRD must add up to 100%, a decrease in one phase must be matched by increases in all of the others.

The anionic surface charge may also play a significant role in the mechanism of this rapid decrease in C_3S. The dissolution of C_3S into solution initially occurs rapidly in water. This dissolution has been suggested to subside when the surface of the C_3S changes, beginning the induction period [16]. While different theories exist about the mechanism of the reduction in the rate of early C_3S dissolution, one by Barret and Menetrier [17] suggests that the dissolution of the C_3S surface results in a net positive charge on the particle. In the bulk cement paste this surface charge is thought to be balanced by hydroxyl ions which block further dissolution until a critical concentration of calcium and silicon is reached. If this were the case, then the negative charge of the air-void surface may neutralize this surface charge and allow C_3S dissolution to continue in this region without an induction period. This would explain the observed rapid decrease in C_3S content in the air void shell. As the C_3S dissolves, an early C–S–H may be nucleating on the air void, giving the shell the physical characteristics observed. With time, the surface charge on the air-void shell is likely reduced from this C–S–H formation, decreasing the ability to control the surface charge of the C_3S and the induction period begins. This would explain the reduced rate of dissolution and the beginning of the induction period for the C_3S.

As explained previously it appears the C_3S is dissolving or leaving the surface of the air-void as all other phases in the analysis are shown to increase. However, the $CaCO_3$ in the analysis showed a much more significant increase compared to the other phases and this increase appears to be proportional to the decrease in C_3S. The cause of this increase is unclear, but they appear related. One possibility is that calcium ions released from the dissolving C_3S may concentrate at the charged air-void shell surface, since it is negatively charged, as discussed earlier. These free calcium ions may react with carbon dioxide that is dissolved in the mixing water, water column used to separate the air-voids from the paste, or from the air contained in the air-void to form the $CaCO_3$. This formation of $CaCO_3$ is likely an artifact of the test setup utilized as it was not observed in the 60 day sample in the SEM investigation. For this mechanism to be satisfactory then the C_3S in cement would need to contribute calcium ions to the formation of $CaCO_3$ and to the formation of other hydration products. This may be possible as the EDXA on the 60 day old air-void shell suggests that the C–S–H formed on the air-void shell has a low calcium content which could allow the remaining calcium ions to contribute to the formation of the $CaCO_3$. It should also be noted that there was no portlandite (CH) in the air-void shell or in the paste during the 2 hour fresh testing period. This is not surprising, since the induction period had not ended and CH generally does not precipitate during this period. Therefore, CH formation is not competing with $CaCO_3$ for calcium ions which would permit it to form.

It was observed in this study that the use of a synthetic AEA resulted in a much more rapid decrease in C_3S content than with the wood rosin AEA and displayed different physical properties. This difference in performance is likely attributable to differences in the chemical nature of the surfactants used in the different AEA products. This could be from differences in surface chemistries that promote the hydration or dissolution of C_3S. However, without detailed knowledge of the nature and concentration of the compounds utilized in these products it is difficult to make comments on their difference in performance. The ability to understand how differences in these surfactants change the performance of the air-void shell is crucial to improving the performance of existing products.

It should be noted that the explanations offered for the changing composition of the air void shells are speculative and it is possible that the chemistry of the shells is controlled by mechanisms other than those suggested here. This is an area that certainly merits further research.

5. Conclusions

This paper presents the results of an investigation into the physical and chemical properties of air-void shells. The results are not meant to be conclusive; a large amount of information remains unknown. However, several new insights have resulted from this work.

- It has been shown that there is a strong adhesion between cement particles and an air-voids surface beginning at the first minutes of hydration.
- It appears that there is a large difference in transparency between the wall of air-entrained and non air-entrained voids.
- There is a significant difference in behavior between the resulting shells with different AEA admixtures when the fluid pressure surrounding voids is increased and then decreased again to atmospheric pressure. Voids made with synthetic AEA sustain no permanent damage, while voids made with Vinsol resin and wood rosin crack on depressurization.
- The cracks in a wood rosin void shell were observed to self-heal.
- The amount of C_3S present in the air-void shell is lower than in the original unhydrated cement and the bulk paste after 8 min of hydration. This effect may be due to delays in the induction period for the C_3S particles at the air-void surface.
- The increase in $CaCO_3$ in the air-void shell in the first 2 h of testing may be an artifact of the sample preparation technique as it was not observed in the SEM analysis of the 60 day old air-void shell.
- The rate of C_3S decrease and $CaCO_3$ increase is more rapid for synthetic AEA than for wood rosin AEA. It is likely that this difference in hydration rate is related to the difference in behavior of the air-void shells of the different AEAs.
- SEM observations and EDXA of the air-voids in the 60-day-old cement paste showed that the surface of the air-void seems to be predominately made up of a C–S–H phase that is of a different morphology than that found in the C–S–H of the bulk paste.

While this paper showed several unique physical characteristics of air-entrained void shells, more work is needed to better characterize the chemical makeup of this material. The majority of the work done in this paper to chemically characterize the air-void shells focused on the crystalline material found in the shell. While the findings are helpful, no data are presented regarding the amorphous materials involved as no analytical techniques are currently readily available to the authors to analyze early amorphous hydration products in these shells. Characterization of the amorphous material is needed before any final conclusions can be drawn. If one were able to fully and accurately characterize the shell material then it may be possible to explain why the AEA voids have their respective physical properties that change with time, pressure, and AEA composition. It may also be possible to engineer new surfactants that could improve the performance of air-entrained concrete.

Acknowledgements

The authors would like to thank the following: Tom Van Dam for his encouragement to investigate the chemical properties of the air bubble shell, Ken Hover for his suggestions and insight, and Doug Hooten for his thoughts and inspiration. Funding for this research was provided by the Portland Cement Association through a graduate fellowship to the lead author and from the Texas Department of Transportation. The following workers served as undergraduate research assistants on this project: Christopher Wolters, Dustin Wilson, Adam Haggerty, Christina Arnaout, and Ryan Rush.

Appendix A. Supplementary data

Supplementary data associated with this article can be found, in the online version, at doi:10.1016/j.cemconres.2009.01.018.

References

[1] Ley, M.T., Folliard, K.J., Hover, K.C., Observations of air-bubbles escaped from fresh cement paste, Cem. Concr. Res., (in press) doi:10.1016/j.cemconres.2009.01.019.
[2] R.C. Mielenz, V.E. Wolkodoff, J.E. Backstrom, H.L. Flack, Origin, evolution, and effects of the air void system in concrete. Part 1—entrained air in unhardened concrete, J. Am. Concr. Inst. 55 (7) (1958) 95–121.
[3] K.C. Hover, Some recent problems with air-entrained concrete, Cem. Concr. Aggregates 2 (1) (1989) 67–72.
[4] F.T. Gay, A factor which may affect differences in the determined air content of plastic and hardened air-entrained concrete, Proceedings of the Fourth International Conference on Cement Microscopy, Int. Cem. Microscopy Assoc., Las Vegas, 1982, pp. 286–292.
[5] V.H. Dodson, Concrete Admixtures, Van Nostrand Reinhold, New York, 1990, pp. 136–143.
[6] M. Pigeon, P. Plante, Study of cement paste microstructure around air voids: influence and distribution of soluble alkalies, Cem. Concr. Res. 20 (1990) 803–814.
[7] A.I. Rashed, R.B. Williamson, Microstructure of entrained air voids in concrete: part I, J. Mater. Res. 6 (9) (1991) 2004–2012.
[8] A.I. Rashed, R.B. Williamson, Microstructure of entrained air voids in concrete: part II, J. Mater. Res. 6 (11) (1991) 2474–2483.
[9] D.J. Corr, J. Lebourgeois, P.J.M. Monteiro, J. Bastacky, E.M. Gartner, Air void morphology in fresh pastes, Cem. Concr. Res. 32 (7) (2002) 1025–1031.
[10] ASTM C 150, Standard Specification for Portland Cement, , 2002.
[11] H. Rietveld, A profile refinement method for nuclear and magnetic structures, J. Appl. Crystallogr. 2 (1969) 65–71.
[12] P.E. Stutzman, Guide for X-ray powder diffraction analysis of Portland Cement and clinker, National Institute of Standards and Technology Internal Report 5755, 1996.
[13] ASTM C 305, Standard Practice for Mechanical Mixing of Hydraulic Cement Pastes and Mortars of Plastic Consistency, , 1999.
[14] B. Ozturk, G. Behin-Aein, B.N. Flanders, Hard-disk behavior and beyond in Langmuir films of CdSe nanoparticles, Langmuir 21 (2005) 4452–4457.
[15] S. Diamond, Cement Paste Microstructure—An Overview at Several Levels, Hydraulic Cement Pastes: Their Structure and Properties, Cem and Concr Assoc, Slough U.K., 1976, pp. 2–30.
[16] E.M. Gartner, J.F. Young, D.A. Damidot, I. Jawed, in: J. Bensted, P. Barnes (Eds.), Hydration of Portland Cement, Structure and Performance of Cements2nd Ed., 2002, pp. 57–108.
[17] P. Barret, D. Menetrier, Filter dissolution of C_3S as a function of the lime concentration in a limited amount of lime water, Cem. Concr. Res. 10 (4) (1980) 521–534.